M&S

PRACTICAL MEASUREMENT STRATEGIES FOR VERIFICATION OF FREEFORM SURFACES USING COORDINATE MEASURING MACHINES

G. Rajamohan, M. S. Shunmugam, G. L. Samuel

Indian Institute of Technology Madras, Department of Mechanical Engineering, , Chennai - 600 036, India
(g.rajamohan@yahoo.co.in, ✉ shun@iitm.ac.in, +91 44 2257 4677, samuelgl@iitm.ac.in)

Abstract

Freeform surfaces have wider engineering applications. Designers use B-splines, Non-Uniform Rational B-splines, etc. to represent the freeform surfaces in CAD, while the manufacturers employ machines with controllers based on approximating functions or splines. Different errors also creep in during machining operations. Therefore the manufactured freeform surfaces have to be verified for conformance to design specification. Different points on the surface are probed using a coordinate measuring machine and substitute geometry of surface established from the measured points is compared with the design surface. The sampling points are distributed according to different strategies. In the present work, two new strategies of distributing the points on the basis of uniform surface area and dominant points are proposed, considering the geometrical nature of the surfaces. Metrological aspects such as probe contact and margins to be provided along the sides have also been included. The results are discussed in terms of deviation between measured points and substitute surface as well as between design and substitute surfaces, and compared with those obtained with the methods reported in the literature.

Keywords: freeform surface, coordinate measuring machine, machining errors, probe size, sampling strategies, substitute geometry

I. Introduction

Freeform features find wider applications in the dies and moulds, patterns and models, plastic products, *etc.* used in many fields ranging from automotive and aerospace to biomedical, entertainment and geographical data processing [1]. Designers use B-splines, Non-Uniform rational B-splines, *etc*. in creating freeform surfaces for engineering applications and often specify profile tolerances. Manufacturers employ machines with controllers based on approximating functions or splines. Also during the machining operations, errors are introduced due to tool deflection, workpiece deflection, guideway errors, spindle runout, machine vibration, *etc*. Therefore, the manufactured freeform surfaces are verified using contact and non-contact methods. The coordinate measuring machines (CMMs) using contact probes measure a large number of discrete sample points. These measured points are used to create the substitute geometry for the feature being measured. The substitute geometry is compared with the design intent (CAD model) to determine conformance. It is intuitive that the measurement accuracy increases with increased sample size, however the sample size is often limited by cost and time constraints. Thus, for a given sample size, the sampling strategy used is expected to determine the locations of these measurement points such that the surface may be effectively characterized.

Verification of freeform features is a challenging task. The common measurement strategy, especially in the inspection planning software, is to distribute the sample points in a uniform pattern [2]. Though the method is very simple, it may often result in inadequate sampling

when there are sharp changes in curvatures and unnecessarily more sampling at relatively flat regions, both of which are undesirable in the measurement process. A number of research efforts to overcome this problem have been reported in the literature. Cho and Kim [3] proposed a sampling method using the surface mean curvature. Their method divides the surface into sub-regions and ranks them according to their mean curvature. A factor called region selection ratio, ranging between 0 and 1, is used in such a way that sample points are spread over the surface for larger region selection ratio and accumulated at the regions of high curvature for smaller region selection ratio. Pahk, *et al.* [4] proposed three sampling methods, viz. uniform distribution, curvature dependent distribution and hybrid distribution. The uniform distribution places sample points in the middle of the surface grid. The curvature dependent distribution uses the normal curvature and places more sample points at regions of high normal curvature. The hybrid method distributes the sample points in a user-specified proportion between the uniform and curvature dependent distribution methods.

Edgeworth and Wilhelm [5] proposed an iterative method based on the surface normal data in which an interpolating curve between sample points on an initially sampled surface is developed and areas requiring further samples are identified for a complete measurement. ElKott, *et al.* [6, 7] proposed four sampling algorithms based on surface feature. The equi-parametric sampling method distributes the sampling points equally along the knot vectors. The patch-size-based sampling method divides the surface into patches at the knot vectors. The share of points along the *u* and *v* parametric directions is proportional to the size of the patch. The patch mean Gaussian curvature method ranks the surface patches on the basis of their mean Gaussian curvature and the share of sample points will be larger for patch with higher ranking. The fourth method combines patch size and mean Gaussian curvature-based methods with user specified weights.

Ainsworth, *et al.* [8] proposed three sampling criteria, namely a chord length criterion specifying the maximum chordal deviation between the line connecting any two points and the surface; a minimum sample density criterion specifying the maximum allowed distance between any two neighboring points on the surface; and a parameterization based sampling criterion taking the number of samples per knot span as specified by the user. Obeidat and Raman [9] proposed three heuristic algorithms for sampling of freeform surface patches using maximum Gaussian curvature, mean Gaussian curvatures and the point with average of the mean Gaussian curvature and minimum Gaussian curvature as critical points. The first algorithm starts with three sample locations in each patch corresponding to the critical points and places additional sample points in low density patches. In the second algorithm, the initial sample points are placed according to the first algorithm and the remaining points are added according to a particular patch size. The third algorithm first allocates sample points using patch mean Gaussian curvature ratio, additional sample points are added according to patch size ratio.

It is seen that different strategies have been reported in the literature for verification of freeform features using a CMM. Given the number of sample points, the sampling strategy has to distribute these points over the surface in such a way that the feature is effectively characterized. At the sample positions, the measurement is carried out and the measured points are used to construct the substitute geometry or surface. The linear and normal deviations of the measured point from substitute surface are shown in Fig. 1. It is observed from the literature that the effect of probe size on the sampling results is not considered, while this is very important as the probe may not make contact with the work surface at the same point as that of the sampling point chosen. Next important observation is that these strategies lack metrological sense, which emphasizes that the sample points cannot be located at the edges as the edge measurement is unreliable. These issues can cause potential changes in the results obtained during verification. The above issues have already been considered by the

authors for freeform profiles [10] and are being extended here to freeform surfaces. Two new surface geometry based sampling strategies have been proposed in the present work. The first strategy is based on the surface area and the second strategy is based on the concept of dominant points. Three existing sampling strategies, namely the uniform distribution in Cartesian space and parametric space and distribution based on patch-size are also implemented. The results obtained using all these five methods are reported and discussed. It is seen that uniform surface area based method performs well in capturing higher form error values with low positional errors.

2. CAD model of freeform surface

The freeform features used in this study use the Non-Uniform Rational B-Splines (NURBS) representation [11]. The NURBS is used here, as it is the de facto industrial standard for computer aided design (CAD) due to its ability to accurately represent various shapes, including the primitives such as the spheres, cylinders, etc. to even very complex freeform features. The CAD model of freeform surface is referred to as design freeform surface or simply design surface in the present work.

The design surface used in this work is a C^2 continuous, Non-uniform Rational B-Spline (NURBS) surface. The NURBS surface is defined using $(n+1)*(m+1)$ control points, denoted as $P_{i,j}$. The NURBS surface with degrees (p, q), defined in parametric space (u, v), is given as:

$$S(u,v) = \frac{\sum_{i=0}^{n} \sum_{j=0}^{m} N_{i,p}(u) N_{j,q}(v) w_{i,j} P_{i,j}}{\sum_{i=0}^{n} \sum_{j=0}^{m} N_{i,p}(u) N_{j,q}(v) w_{i,j}}; \quad u, v \in [0,1].$$

(1)

The $\{P_{i,j}\}$ are the control points forming a bidirectional control net, the $\{w_{i,j}\}$ are the weights and $\{N_{i,p}(u)\}$ and $\{N_{j,q}(v)\}$ are the non-rational B-spline basis functions defined in the knot vectors U and V respectively. The value of $N_{i,p}(u)$ can be estimated using the following recursive relations, choosing $0/0 = 0$, if the denominators in the equation become zero.

$$N_{i,p}(u) = \frac{u - u_i}{u_{i+p} - u_i} N_{i,p-1}(u) + \frac{u_{i+p+1} - u}{u_{i+p+1} - u_{i+1}} N_{i+1,p-1}(u),$$

(2)

where, $N_{i,0}(u) = $ $1;$ $u_i \le u < u_{i+1}$
                   $0;$ otherwise

The above equation can be used to compute $N_{j,q}(v)$ by appropriately replacing the variables.

The data used for designing the example surface is given below.

Surface degrees (p, q): 3, 3 Number of control points $((n+1) * (m+1))$: 5 * 5
Control points (mm):
$P_{0,0}(0, 0, 20)$ $P_{0,1}(0, 12.5, 30)$ $P_{0,2}(0, 25, 33)$ $P_{0,3}(0, 37.5, 20)$ $P_{0,4}(0, 50, 25)$
$P_{1,0}(12.5, 0, 23)$ $P_{1,1}(12.5, 12.5, 27)$ $P_{1,2}(12.5, 25, 30)$ $P_{1,3}(12.5, 37.5, 17)$ $P_{1,4}(12.5, 50, 23)$
$P_{2,0}(25, 0, 25)$ $P_{2,1}(25, 12.5, 25)$ $P_{2,2}(25, 25, 27)$ $P_{2,3}(25, 37.5, 22)$ $P_{2,4}(25, 50, 25)$
$P_{3,0}(37.5, 0, 20)$ $P_{3,1}(37.5, 12.5, 27)$ $P_{3,2}(37.5, 25, 20)$ $P_{3,3}(37.5, 37.5, 20)$ $P_{3,4}(37.5, 50, 14)$
$P_{4,0}(50, 0, 27)$ $P_{4,1}(50, 12.5, 23)$ $P_{4,2}(50, 25, 25)$ $P_{4,3}(50, 37.5, 27)$ $P_{4,4}(50, 50, 22)$
Knot vectors: $U = \{0.0, 0.0, 0.0, 0.0, 0.3600, 1.0, 1.0, 1.0, 1.0\}$
               $V = \{0.0, 0.0, 0.0, 0.0, 0.3717, 1.0, 1.0, 1.0, 1.0\}$

Fig. 2 shows the design freeform surface. The design surface is discretized in Cartesian space with suitable Δx and Δy spacing along the x and y axes. The corresponding u and v parameter values at each point on Cartesian space are computed. The mean curvature (H) and Gaussian curvature (K) are also computed [12] using the following equations.

$$H = \frac{EN - 2FM + GL}{2(EG - F^2)}; \quad K = \frac{LN - M^2}{(EG - F^2)}, \tag{3}$$

$$E = \vec{S}_u \bullet \vec{S}_u; \quad F = \vec{S}_u \bullet \vec{S}_v; \quad G = \vec{S}_v \bullet \vec{S}_v; \quad L = \vec{n} \bullet \vec{S}_{uu}; \quad M = \vec{n} \bullet \vec{S}_{uv}; \quad N = \vec{n} \bullet \vec{S}_{vv}; \quad \vec{n} = \frac{\vec{S}_u \times \vec{S}_v}{\left| \vec{S}_u \times \vec{S}_v \right|},$$

where, S_u is the first derivative along u; S_v is the first derivative along v; S_{uu} is the second derivative along u; S_{uv} is the derivative of S_u along v and S_{vv} is the second derivative along v. The symbols $\times$ and $\bullet$ indicate the cross and dot products respectively.
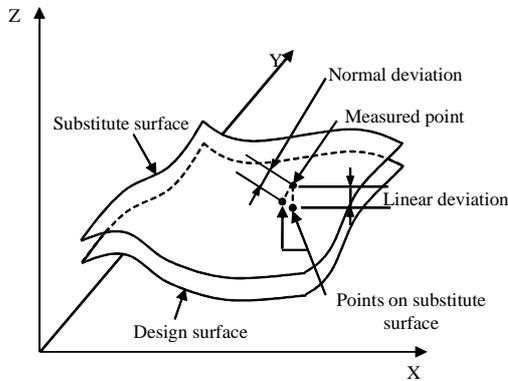

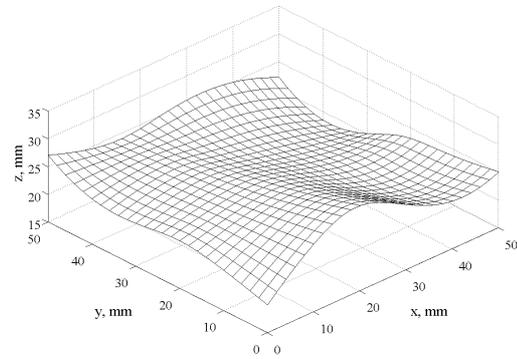Fig. 1. Freeform surface showing the measured point and deviations.

Fig. 2. 3-D plot of the design surface.

3. Measurement strategies

In the present work, performance of all the reported algorithms is analyzed with 5% margins from all boundaries/edges. The start and end points are set at 5% of the feature size along that direction in Cartesian space. For this margin, the lower and upper bounds of the surface along the x-axis, denoted as x_{min} and x_{max} respectively, are computed. The corresponding parameter values are u_{min} and u_{max} respectively. Similarly, the lower and upper bounds of the surface along the y-axis, denoted as y_{min} and y_{max} respectively, are computed. The corresponding parameters values are v_{min} and v_{max} respectively. The general flowchart for all measurement strategies is shown in Fig. 3.

3.1. Existing methods

3.1.1. Uniform distribution in Cartesian space

The sample points are distributed with nearly equal spacing along the x and y axes. The spacing between sample points along each axis depends on the feature size and the number of sampling points along that axis. Then, the positions (x^*_i, y^*_j) of all the sampling points can be obtained from the equation given below.

$$x_i^* = x_{\min} + (i-1)\frac{x_{\max} - x_{\min}}{(N_u - 1)}; i = 1,...,N_u \text{ and } y_j^* = y_{\min} + (j-1)\frac{y_{\max} - y_{\min}}{(N_v - 1)}; j = 1,...,N_v, \quad (4)$$

where N_u and N_v are the sample sizes along the x and y axes respectively. Using the computed (x_i^*, y_j^*) values, the nearest point (x_i, y_j) on the discretized surface is obtained. The sample points thus obtained are shown in Fig. 4a.
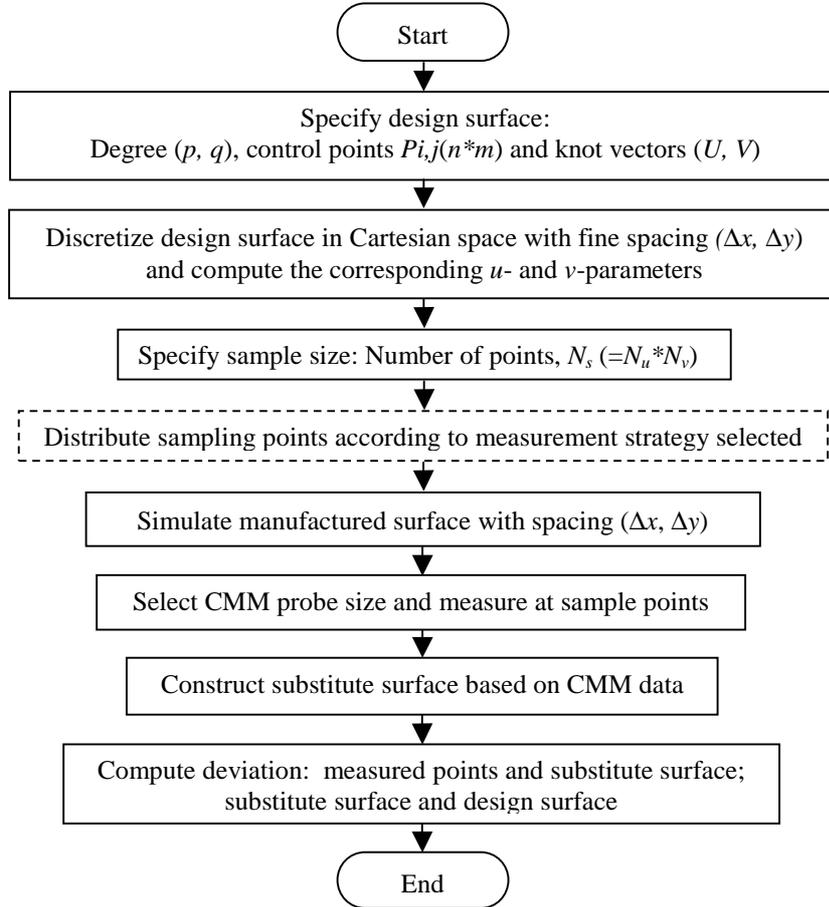

Fig. 3. General flowchart for the present work.

3.1.2. *Uniform distribution in parametric space*

The sample points are distributed with nearly equal spacing along the u and v parametric directions. The spacing between sample points along each parametric direction depends on the range of the parameter and the number of sampling points along that direction. The positions of sample points (u_i^*, v_j^*) are given by the following equation:

$$u_i^* = u_{\min} + (i-1)\frac{u_{\max} - u_{\min}}{(N_u - 1)}; i = 1,...,N_u \text{ and } v_j^* = v_{\min} + (j-1)\frac{v_{\max} - v_{\min}}{(N_v - 1)}; j = 1,...,N_v, \quad (5)$$

where N_u and N_v are the sample sizes along the u and v directions respectively. The computed (u_i^*, v_j^*) values are used to select the nearest points (u_i, v_j) from the discretized design surface. The sample points obtained by this method are shown in Fig. 4a.

3.1.3. Distribution based on patch size

The patch size ranking strategy proposed by Obeidat and Raman [9] is suitably modified to work for a given sample size. The knot vectors (*U, V*) are used to divide the given design surface into patches and the patch sizes are computed. If a patch has *u* bounds as u_1 and u_2 and *v* bounds as v_1 and v_2, the patch size is computed as $(u_2 - u_1) * (v_2 - v_1)$. The given sample size N_s is shared among the patches based on their sizes. The selection of sample points is based on mean Gaussian curvatures (*K*). The points are selected in the order of K_{max}, K_{avg1}, $K_{avgmin1}$, *etc*. The Gaussian curvatures are computed as:

$$K_{avg1} = (K_{max} + K_{min})/2; \quad K_{avg2} = (K_{avg1} + K_{max})/2; \quad K_{avgmin1} = (K_{avg1} + K_{min})/2$$

$$K_{avgmin2} = (K_{avgmin1} + K_{min})/2; \quad K_{avgmin3} = (K_{avgmin2} + K_{min})/2. \tag{6}$$

3.2. Proposed methods

3.2.1. Distribution based on surface area

The proposed method starts with computation of surface area (A_t) by approximating the design surface to consist of planar triangular facets obtained using the discretized data. The total surface area is obtained as:

$$A_t = \sum_{k=0}^{N-1} \sum_{l=0}^{M-1} (\Delta_{k,2l} + \Delta_{k,2l+1}),$$
$$\tag{7a}$$

where $\Delta_{k,2l}$ is the area of a triangle with vertices at [(*k, l*), (*k*+1, *l*) and (*k*+1, *l*+1)], $\Delta_{k,2l+1}$ is the area of a triangle with vertices at [(*k, l*), (*k, l*+1) and (*k*+1, *l*+1)] and (*N* + 1), (*M* + 1) are the number of points on the discretized surface along the x and y directions respectively. The area per sample point is computed as:

$$A_p = \frac{A_t}{(N_u - 1)(N_v - 1)},$$
$$\tag{7b}$$

where, N_u and N_v are the number of sample points along the respective axes. Starting from ($x_i = x_{min}$, $y_j = y_{min}$), the (x_{i+1}, y_{j+1}) values are selected such that the aspect ratio between the *x* and *y* axes are maintained and at the same time the surface area between (x_i, y_j) and (x_{i+1}, y_{j+1}) is nearly equal to A_p, with *i* varying from 1,…,(N_u−1) and *j* varying from 1,…,(N_v−1). The sample points thus obtained are shown in Fig. 4b.

3.2.2. Distribution based on dominant points

The points on a freeform surface with maximum local mean curvature are identified as dominant points [13]. The computation of curvatures is outlined in Section 2. Along with these points, four points defining the corners of the surface are taken to obtain the initial sample set. The initial sample points are used to form regions on the surface in Cartesian space. Additional sample points are added one at a time, starting with the largest region in terms of surface area. The sample point is taken to be nearly mid-point of the region. After adding the point, the region is divided into four sub-regions. The procedure is continued until the required sample size is obtained. Fig. 4b shows the sample points in this case.
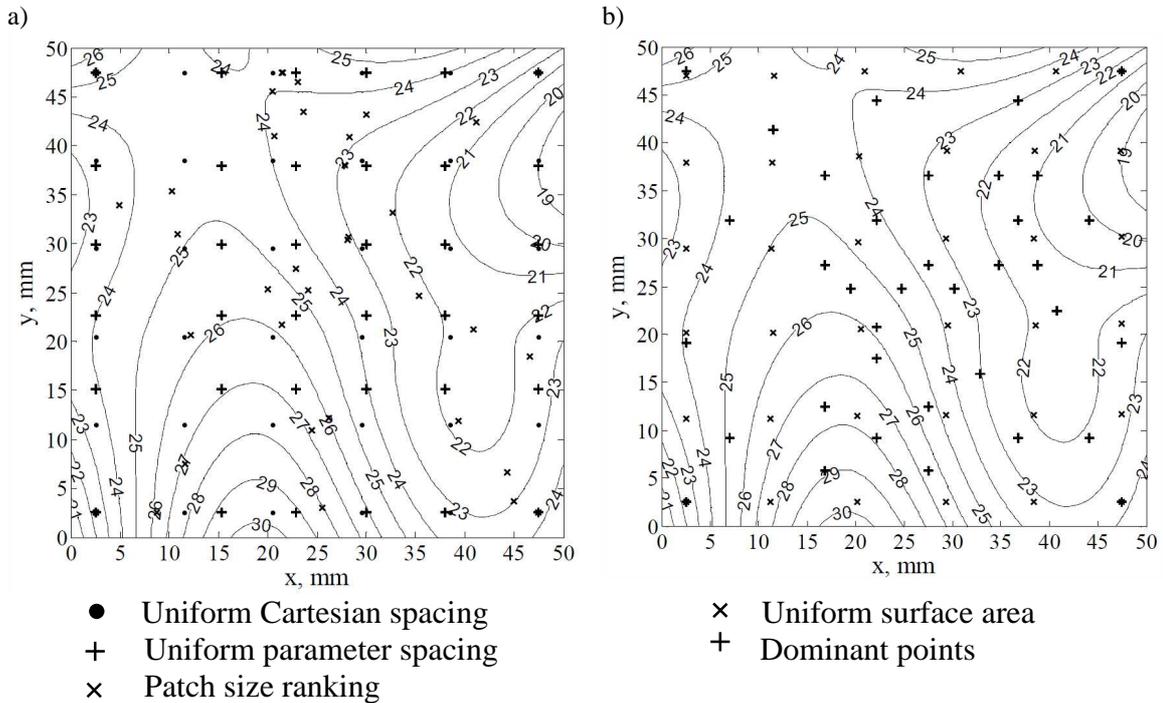
Fig. 4. Sample positions on surface (sample size, 36 = 6x6) with 5% margin. a) Existing methods.
b) Proposed methods.

4. Simulation of manufacturing errors

In general engineering practice, two types of errors such as systematic error and random error are encountered. The systematic errors follow a particular, identifiable pattern so that they can be accounted for more precisely. The random errors do not have any identifiable pattern and hence can be assumed to follow certain probability distribution. Both these types of errors are considered here for simulating the manufactured surfaces.

4.1. Systematic errors

Systematic errors consist of different wavelengths. The long wavelength errors come from various sources such as errors in machine tool guideways, deflection of workpiece, *etc*., while other wavelength errors are due to vibrations, changing curvatures of surface machined, *etc.* The effect of these errors can be simulated by using appropriate mathematical functions [14].

4.1.1. Quadratic form error (δ_q)

The quadratic error, representing the error of form, can be approximated using a second-order polynomial as given in Eq. (8).

$$\delta_q = b_0 + b_1 x + b_2 y + b_3 xy + b_4 x^2 + b_5 y^2,$$

(8)

where, b_0, b_1, b_2, b_3, b_4, and b_5 are the coefficients of the second-order polynomial. In the present work, $b_0 = 4.5(10^{-3})$, $b_1 = b_2 = -1.7(10^{-4})$, $b_3 = -4.5(10^{-6})$ and $b_4 = b_5 = 3.7(10^{-6})$ are taken to get a maximum value of δ_q as 0.0105 mm.

4.1.2. Sinusoidal form error (δ_s)

The sinusoidal form error can be approximated using a combination of sinusoidal functions as given below:

$$\delta_s = A\sin(w_x x + w_y y) + B\cos(w_x x + w_y y), \tag{9}$$

where, w_x is given by $2\pi/\lambda_x$ and w_y is given by $2\pi/\lambda_y$; λ_x and λ_y are wavelengths of sinusoidal components along the x and y direction respectively. The amplitudes of sine and cosine components A and B are taken to be 0.005 mm. The wavelengths can be assigned values of 1, 2 and 3 to simulate different sinusoidal form errors. The maximum value of this error component (δ_s) is 0.010 mm.

4.1.3. Machining form error (δ_m)

When the cutting tool encounters changing machining conditions as in the case of machining of different curvatures in a given surface, form errors are introduced. The machining error distribution is computed on the basis of the mean curvature as shown below:

$$\delta_m = f_s(i_s - 0.5), \tag{10}$$

where, f_s is the maximum machining error. Index i_s based on mean curvature of the surface is given by $i_s = (H - H_{min})/(H_{max} - H_{min})$. The terms H, H_{min} and H_{max} are the mean curvature, minimum mean curvature and maximum mean curvature of the surface respectively. A value of 0.010 mm is chosen for f_s so that the maximum value of this error component (δ_m) is 0.010 mm.

4.2. Random error (δ_c)

The random errors in a machining process can be obtained by appropriately conducting a machine capability study. This error may be added to systematic errors and the measurement can be simulated. During the measurement, noise due to the measuring instrument also gets added. The information about relevant range of variation for this random error component can be obtained from the CMM manufacturer's calibration chart.

The random errors have to be lower than the systematic errors. Since the systematic error components used in the present research have been limited to about 0.010 mm, the random error has to be less than this value. The present work represents the random errors (δ_c) due to machining and measurement processes by a normal distribution with a mean value of 0.0 mm and standard deviation of 0.001 mm, so that the total value of δ_c is about 0.006 mm.

4.3. Combined manufacturing error

The combined manufacturing error is obtained by superimposing all the error components on the design surface. Fig. 5 shows a 3-D plot of combined errors and the maximum linear error introduced is 25.29 µm. If $S(x_i, y_j, z_{i,j})$ is any sample point on the design surface and its coordinates on the manufactured surface are represented by $S_m(x_i, y_j, z_{i,j}')$, then $z_{i,j}'$ is given by $(z_{i,j}+\delta_q+\delta_s+\delta_m+\delta_c)$. The coordinates $S_m(x_i, y_j, z_{i,j}')$ have to be used for arriving at probe contact during a CMM measurement.

5. Computation of probe contact point

In view of the manufacturing errors present on the freeform features, the probes make contact with the feature at points different from the sample points chosen [10]. Hence, computing the measurement errors based on sample points alone may lead to erroneous results. Therefore, the actual point of contact of the probe with the feature needs to be established first.

Lingadurai and Shunmugam extended a general method to computing the envelope of a circle rolling over the profile [15] to compute the three dimensional envelope using a toroidal element [16]. In this paper, the computation of probe contact for freeform surfaces is done using a hemispherical element in place of toroidal element. This approach requires discretization of bottom half of the probe (hemispherical shape) to the same discretization spacing, namely Δx and Δy (Fig. 6) and the ordinate data for the probe $(E_{k,l})$ at different sections are to be computed.

The CMM measurement is simulated by positioning the probing system over the freeform surface such that the sample point (x_i, y_j) coincides with the centre of probe $(E_{0,0})$. The probe is then moved steadily downwards until it makes contact with the manufactured surface. For computing the probe contact point, the sum of the probe and surface ordinates $(E_{k,l}+z'_{i,j})$ is computed within the region of interest. The point at which the maximum value of this sum (z_{max}) occurs gives the probe contact point (x_c, y_c) with the surface. This procedure is repeated for all sample points to get the measurement data $\{S_c\}$.
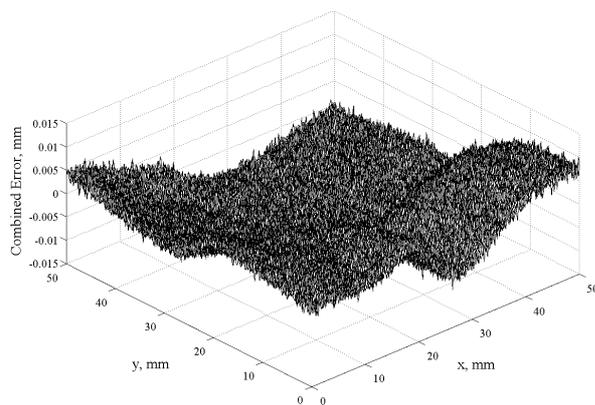

Fig. 5. 3-D plot of combined error (Quadratic error + Sinusoidal ($\lambda_x=\lambda_y=1$) error + Machining error + Random).
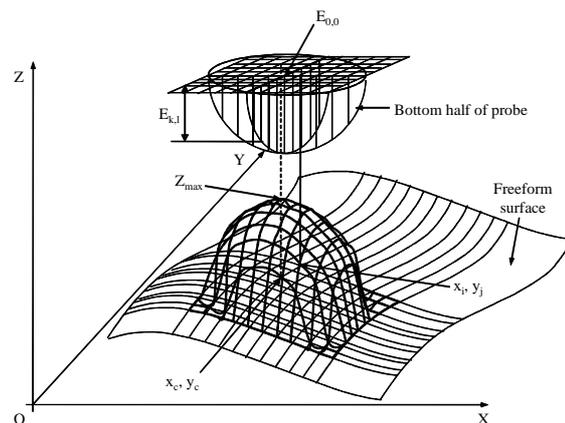
Fig. 6. Probe contact point.

6. Substitute surface and computation of deviations

6.1 Substitute surface

The degrees, knot vectors, number of control points and their weights of the substitute surface are taken to be as those of the design surface. Let $\{S_c\}$ consist of a set of N_s measured points and $\{\bar{u}_l, \bar{v}_l\}$, $l=1,\dots,N_s$ be the corresponding location parameters in u-v space. The objective is to fit a substitute NURBS surface with N=$[(n+1)*(m+1)]$ control points, represented as:

$$S_s(\overline{u},\overline{v}) = \frac{\sum_{i=0}^{n}\sum_{j=0}^{m} N_{i,p}(\overline{u})N_{j,q}(\overline{v})w_{i,j}P_{i,j}}{\sum_{i=0}^{n}\sum_{j=0}^{m} N_{i,p}(\overline{u})N_{j,q}(\overline{v})w_{i,j}}; \quad \overline{u},\overline{v} \in [0,1].$$

(11)

A two-step linear approach is reported in the literature for fitting of NURBS surfaces. In the first step, the weights are identified and the control points are computed in the second step [17]. Since the weights are taken to be 1.0, it reduces to a single-step procedure and the algorithmic detail for computing the control points is given in Appendix-A.

6. 2. Computation of deviations

The deviation of a measured point from the substitute surface is computed in the vertical (linear) and normal directions as shown in Fig.1. The distance between the measured point and corresponding point on the substitute surface along the *z*-axis gives the linear deviation. The shortest distance between the measured point and the substitute surface represents the normal deviation. Let e_i represent the deviation and (e_{max}, e_{min}) denote the maximum and minimum values of the deviations respectively. The form error is taken to be deviation of the measured points from the substitute surface and it is computed as:

$$\Delta_s = |e_{max} - e_{min}|.$$

(12)

Depending on the nature of the deviations considered, the form error Δ_s may be expressed as a linear or normal value.

The substitute surface established from the measured points may also be positioned differently with reference to the design surface. The deviations between the substitute and the design surfaces are computed on a point-to-point basis as linear or normal values following the procedure outlined above. For quantifying this error, the maximum and minimum deviations are represented by p_{max} and p_{min}. The form and positional error values are given in Table 1 for different measurement strategies.

7. Results and discussion

The NURBS surface taken for the present work is a multi-patch surface with data as given in Section 2. The example surface shows substantial variation in its geometry (Fig. 2) and different measurement strategies shown in Fig. 3 can be applied conveniently. The surface is more suitable for an algorithm involving patch-size ranking as suggested by Obeidat and Raman [9]. One can easily visualize the nature of the example surface using contour plots given in Fig. 4 and the distribution of sample points. The distribution of sample points based on uniform Cartesian and parametric spacing leads to a more ordered scheme which is independent of the geometric nature of the surface. The uniform surface area method is giving slightly better distribution which depends to some extent on the surface geometry. The strategies based on patch size ranking and dominant points show much better distribution of sample points with a smaller number of points in flatter regions.

At the sample positions, data corresponding to CMM measurement is obtained on the manufactured surface which represents superimposed systematic and random errors on the design surface. The contact points are determined using the procedure outlined in Section 5. The probe sizes are assumed to be 0.0 and 1.0 mm in this paper. Using the measured points, the substitute surface is established by the procedure given in Appendix A. The linear and normal deviations of the measured points from the substitute surface are computed and the

form error (e_{max}) is arrived at using Eq. (12). Similarly, the deviations of the substitute surface from the design surface are computed to arrive at positional errors, p_{max} and p_{min}. The form and positional error values obtained for different measurement strategies and sample sizes are included in Table 1.

Table 1 Results obtained by different measurement strategies for freeform surfaces (Control points: 5*5) with 5% margin and discretization interval of $\Delta x = \Delta y = 100$ µm. a) Linear error (µm). b) Normal error (µm).

a)

Errors consi-dered	Error intro-duced (µm)	Sample size	Existing Methods						Proposed Methods			
			Uniform Cartesian		Uniform Parameter		Patch Size Rank		Uniform Surface Area		Dominant Points	
			Form Error	Pos. Error	Form Error	Pos. Error	Form Error	Pos. Error	Form Error	Pos. Error	Form Error	Pos. Error
Probe diameter: 0.0 mm												
All Errors ($\lambda_x=\lambda_y=1$)	19.31	36 (6x6)	5.83	+8.63 -12.28	3.52	+8.74 -11.23	2.51	+9.45 -30.81	6.40	+8.90 -11.58	3.26	+12.38 -14.14
All Errors + Random	25.29		4.80	+9.18 -11.01	4.80	+9.60 -12.59	2.72	+8.66 -29.71	7.67	+9.68 -13.55	3.57	+11.98 -17.48
All Errors ($\lambda_x=\lambda_y=1$)	19.31	64 (8x8)	6.37	+8.75 -11.23	6.22	+8.86 -11.19	3.57	+14.76 -22.41	6.66	+8.92 -10.81	4.28	+8.70 -11.92
All Errors + Random	25.29		6.45	+9.22 -10.81	7.18	+10.19 -11.83	4.96	+12.56 -20.73	7.72	+9.65 -10.98	5.27	+10.17 -11.27
Probe diameter: 1.0 mm												
All Errors ($\lambda_x=\lambda_y=1$)	19.31	36 (6x6)	6.03	+8.44 -12.00	3.62	+7.99 -11.13	2.63	+9.25 -29.15	6.52	+8.88 -11.63	3.25	+12.60 -14.19
All Errors + Random	25.29		7.26	+9.57 -11.36	4.65	+8.81 -11.94	4.04	+11.25 -35.13	6.19	+9.27 -11.65	3.45	+18.70 -12.45
All Errors ($\lambda_x=\lambda_y=1$)	19.31	64 (8x8)	6.34	+8.57 -11.08	6.11	+8.62 -10.99	3.65	+14.58 -21.80	6.72	+8.92 -10.83	4.25	+8.74 -11.79
All Errors + Random	25.29		6.13	+9.21 -12.26	6.94	+9.10 -11.95	4.71	+13.01 -36.63	9.76	+8.96 -11.02	5.72	+9.73 -11.31

b)

Errors consi-dered	Error intro-duced (µm)	Sam-ple size	Existing Methods						Proposed Methods			
			Uniform Cartesian		Uniform Parameter		Patch Size Rank		Uniform Surface Area		Dominant Points	
			Form Error	Pos. Error	Form Error	Pos. Error	Form Error	Pos. Error	Form Error	Pos. Error	Form Error	Pos. Error
Probe diameter: 0.0 mm												
All Errors ($\lambda_x=\lambda_y=1$)	18.78	36 (6x6)	5.25	+8.18 -12.22	3.21	+8.23 -11.15	2.44	+8.99 -28.94	5.93	+8.46 -11.46	3.13	+11.79 -12.76
All Errors + Random	24.62		4.31	+8.73 -10.75	4.27	+9.06 -12.51	2.72	+8.22 -27.82	7.12	+9.19 -13.43	3.52	+11.41 -15.80
All Errors ($\lambda_x=\lambda_y=1$)	18.78	64 (8x8)	5.65	+8.30 -11.17	5.79	+8.39 -11.12	3.47	+14.07 -20.53	6.19	+8.47 -10.71	4.06	+8.27 -11.03
All Errors + Random	24.62		6.03	+8.77 -10.76	6.90	+9.65 -11.52	4.89	+11.96 -19.06	7.15	+9.16 -10.85	5.12	+9.20 -11.11
Probe diameter: 1.0 mm												
All Errors ($\lambda_x=\lambda_y=1$)	18.78	36 (6x6)	5.41	+8.02 -11.92	3.35	+7.59 -11.02	2.49	+8.79 -27.44	6.05	+8.43 -11.51	3.12	+12.01 -12.81
All Errors + Random	24.62		6.56	+9.10 -11.27	4.57	+8.37 -11.82	3.81	+10.70 -32.05	5.74	+8.80 -11.49	3.31	+17.84 -11.17
All Errors ($\lambda_x=\lambda_y=1$)	18.78	64 (8x8)	5.62	+8.14 -10.99	5.72	+8.19 -10.89	3.55	+13.90 -19.99	6.26	+8.47 -10.72	4.04	+8.31 -11.02
All Errors + Random	24.62		5.90	+8.75 -12.16	6.80	+8.69 -11.23	4.52	+12.39 -33.56	9.10	+8.96 -11.02	5.44	+8.85 -10.66

Table 1a gives form and positional errors based on linear deviation (*i.e.* along *z*-axis). With all errors, namely systematic and random, combined, the total manufacturing error is 25.29 µm. With a probe diameter of 0.0 mm and sample size of 36 (6x6), the uniform surface area method is able to capture a maximum form error of 7.67 µm when all the errors are present. Without random error added, again the uniform surface area method is able to capture 6.40 µm. In terms of positional error, the uniform surface area method is one among the three

methods (uniform Cartesian: 9.18 + 11.01 = 20.19 μm, uniform parametric: 9.60 + 12.59 = 22.19 μm and uniform surface area: 9.68 + 13.55 = 23.23 μm) yielding lower values, when all errors are present. The same is true when only systematic error is present. When the sample size is increased to 64 (8x8), Table 1(a) shows that higher form error values are captured and the positional errors are reduced.

With a probe of 1.00 mm diameter and larger sample size of 64 (8x8), the uniform surface area method captures the highest form error value of 9.76 μm and lowest positional error of 19.98 (*i.e.* 8.96 + 11.02) μm.

The form and positional error values based on linear deviations are given in Table 1b. It may be seen that the total error on the manufactured surface is 24.62 μm considering the normal direction, while it is 25.29 μm in the linear direction. The values of form and positional errors are also reduced in the normal direction, but the relative performance of the measurement strategies remains the same as that seen in the linear direction.

8. Conclusions

This paper deals with practical aspects of verifying freeform surfaces with a CMM. The measurement margins and probe size have been considered in the present work. Two measurement strategies based on uniform distribution in Cartesian and parametric space yield ordered sample points irrespective of the nature of surface geometry. Other three strategies viz. patch size ranking, uniform surface area and dominant points based methods consider the geometric nature of the surface. The possible manufacturing errors have been added to the design surface and data points corresponding to the measurement using a CMM have been arrived at for different sampling methods by considering the probe contact.

Even though the distribution of points with uniform surface area based method is slightly better than those using uniform Cartesian and parametric spacing methods, it exhibits superior performance in terms of capturing higher form error values with low positional error.

The present study can be extended to cover freeform surfaces of varying complexities and the performance of the different measurement strategies can be further evaluated.

Appendix – A

Construction of Substitute Surface

Taking $\{S_c\}$ as a set of N_s measured points and $\{\bar{u}_l, \bar{v}_l\}$, $l=1,…,N_s$ will be the corresponding location parameters in $u-v$ space. To fit a substitute surface, the NURBS surface with N=$[(n+1)*(m+1)]$ control points is taken [17] as:

$$S_s(\bar{u},\bar{v}) = \frac{\sum_{i=0}^{n}\sum_{j=0}^{m} N_{i,p}(\bar{u})N_{j,q}(\bar{v})w_{i,j}P_{i,j}}{\sum_{i=0}^{n}\sum_{j=0}^{m} N_{i,p}(\bar{u})N_{j,q}(\bar{v})w_{i,j}} ; \quad \bar{u},\bar{v}\in[0,1] \quad \cdot \tag{13}$$

After rearranging the terms on the left and right hand sides, the above equation (13) can be compactly written in matrix form as:

$$BX = \bar{X}Bw; \quad BY = \bar{Y}Bw; \quad BZ = \bar{Z}Bw, \tag{14}$$

where:

$$B = \begin{bmatrix} N_{0,p}(\overline{u}_1)N_{0,q}(\overline{v}_1) & . & . & . & N_{n,p}(\overline{u}_1)N_{m,q}(\overline{v}_1) \\ . & & . & . & . & . \\ . & & . & . & . & . \\ . & & . & . & . & . \\ N_{0,p}(\overline{u}_{N_s})N_{0,q}(\overline{v}_{N_s}) & . & . & . & N_{n,p}(\overline{u}_{N_s})N_{m,q}(\overline{v}_{N_s}) \end{bmatrix};$$

$$X = \begin{bmatrix} X_1 & ... & X_N \end{bmatrix}^T = \begin{bmatrix} w_1 x_1 & ... & w_N x_N \end{bmatrix}^T; \quad Y = \begin{bmatrix} Y_1 & ... & Y_N \end{bmatrix}^T = \begin{bmatrix} w_1 y_1 & ... & w_N y_N \end{bmatrix}^T;$$

$$Z = \begin{bmatrix} Z_1 & ... & Z_N \end{bmatrix}^T = \begin{bmatrix} w_1 z_1 & ... & w_N z_N \end{bmatrix}^T; \quad w = \begin{bmatrix} w_1 & ... & w_N \end{bmatrix}^T;$$

$$\overline{X} = Diag\begin{bmatrix} x'_1 & ... & x'_{N_s} \end{bmatrix}; \quad \overline{Y} = Diag\begin{bmatrix} y'_1 & ... & y'_{N_s} \end{bmatrix}; \quad \overline{Z} = Diag\begin{bmatrix} z'_1 & ... & z'_{N_s} \end{bmatrix}, \quad (15)$$

$\{x_k, y_k, z_k\}$ are the control points in Cartesian space and $\{x_l^{'}, y_l^{'}, z_l^{'}\}$ are the measured points. The control points can be obtained by estimating the weights matrix w. Taking all the weights to be equal to 1, the control points can be obtained by solving (14) in homogenous space. The coordinates of the control points in Cartesian space can be computed as:

$$x_k = X_k/w_k \; ; \; y_k = Y_k/w_k \; ; \; z_k = Z_k/w_k; \qquad \text{for } k=1,..,N. \qquad (16)$$

References

[1] Li, Y., Gu, P. (2004). Freeform surface inspection techniques - state of the art review. *Computer Aided Design*, 36(13), 1395-1417.

[2] ElKott, D.F., Veldhuis, S.C. (2005). Isoparametric line sampling for the inspection planning of sculptured surfaces. *Computer Aided Design*, 37, 189-200.

[3] Cho, M.W., Kim, K. (1995). New inspection planning strategy for sculptured surfaces using coordinate measuring machine. *International Journal of Production Research*, 33(2), 427-444.

[4] Pahk, H.J., Jung, M.Y., Hwang, S.W., Kim, Y.H., Hong, Y.S., Kim, S.G. (1995). Integrated precision inspection system for manufacturing of moulds having CAD defined features. *International Journal of Advanced Manufacturing Technology*, 10, 198-207.

[5] Edgeworth, R., Wilhelm, R.G. (1999). Adaptive sampling for coordinate metrology. *Precision Engineering*, 23, 144-154.

[6] ElKott, D.F., ElMaraghy, H.A., Nassef, A.O. (1999). Sampling for freeform surfaces inspection planning. In *Proceedings of ASME Design Engineering Technical Conference*. Nevada, 1-9.

[7] ElKott, D.F., ElMaraghy, H.A., ElMaraghy, W.H. (2002). Automatic sampling for CMM inspection planning of freeform surfaces. *International Journal of Production Research*, 40(11), 2653-2676.

[8] Ainsworth, I., Ristic, M., Brujic, D. (2000). CAD-based measurement path planning for freeform shapes using contact probes. *International Journal of Advanced Manufacturing Technology*, 16, 23-31.

[9] Obeidat, S.M., Raman, S. (2009). An intelligent sampling method for inspecting freeform surfaces. *International Journal of Advanced Manufacturing Technology*, 40, 1125-1136.

[10] Rajamohan, G., Shunmugam, M.S., Samuel, G.L. (2011). Effect of probe size and measurement strategies on freeform profile deviations using coordinate measuring machine. *Measurement*, 44(5), 832-841.

[11] Piegl, L., Tiller, W. (1997). The NURBS Book. Berlin: Springer-Verlag.

[12] Rogers, D.F., Adams, J.A. (2002). Mathematical Elements for Computer Graphics. New Delhi: Tata McGraw-Hill Pub. Co. Ltd.

[13] Park, H., Lee, J.H. (2007). B-spline curve fitting based on adaptive curve refinement using dominant points. *Computer Aided Design*, 39(6), 439-451.

[14] Kumar, J., Shunmugam, M.S. (2006). Fitting of reference surfaces for engineering surfaces by non-linear least squares technique. *ASME Journal of Computing and Information Science in Engineering*, 6(4), 349-354.

[15] Shunmugam, M.S., Radhakrishnan, V. (1976). Comparison of difference methods for computing the two-dimensional envelope for surface finish measurements. *Computed Aided Design*, 8(2), 89-93.

[16] Lingadurai, K., Shunmugam, M.S. (2005). Use of morphological closing filters for three-dimensional filtering of engineering surfaces. *Journal of Manufacturing Systems*, 24(4), 366-376.

[17] Ma, W., Kruth, J.P. (1998). NURBS curve and surface fitting for reverse engineering. *International Journal of Advanced Manufacturing Technology*, 14, 918-927.